Applied Radiation and Isotopes 67 (2009) 281–286

Contents lists available at ScienceDirect

Applied Radiation and Isotopes

journal homepage: www.elsevier.com/locate/apradiso

Discussion

Monte Carlo calculations of electrons in aluminum

Asuman Aydın

Department of Physics, Faculty of Sciences and Literature, Balikesir University, 10145 Balikesir, Turkey

ARTICLE INFO

Article history:
Received 8 January 2007
Received in revised form
11 March 2008
Accepted 29 April 2008

Keywords:
Monte Carlo
Electron
Transmission
Backscattering
Energy and angular distributions
Aluminum

ABSTRACT

The interaction of keV electrons with solids was studied by considering electrons transmitted through thin films as well as electrons backscattering from semi-infinite solid targets. The elastic scattering cross-section was obtained from the Rutherford differential cross-section. The numerical coefficient in the atomic screening parameter and spin-relativistic correction factor were taken as variables. The inelastic scattering model was employed to simulate the energy loss using Gryzinski's semi-empirical expression and Gryzinski and Liljequist models to calculate the total inelastic scattering cross-section. The simulation results were found to be in good agreement with other simulations and experiments.

1. Introduction

In measurements of electrons traversing matter it is important to know the transmission through that medium, their path lengths and angular distribution through matter. This allows one to seek the improvement of keV electrons-based techniques including medical applications and materials irradiation.

Both elastic and inelastic scattering processes are important in determining, for example, particle ranges, transmission and backscattering probabilities. The Monte Carlo method has been widely accepted as one of the most basic approach to study the penetration of keV electrons and positrons in solids. In this method, the individual particle trajectories resulting from a series of random scattering events are modelled as random walks and simulated in the computer. Monte Carlo simulation can be used to interpret surface-related experiments, which includes electron–solid interaction. It is also considered as a convenient and reliable way of comparing the calculated scattering cross-section with the experiment. It is well known that the accuracy of the Monte Carlo method is strongly related with the modelling of the scattering processes, which depend on the particle energy employed in the simulation. The dominant processes are elastic scattering of individual atoms and inelastic scattering involving core and valance electron excitations.

We have previously developed an analog Monte Carlo code simulating the positron degradation in aluminum (Özmutlu and Aydin,1994). Using this code the transmission and backscattering probabilities,and mean penetration depths were calculated for positrons (Özmutlu and Aydin,1994). In this work, the Monte Carlo code calculations were improved and employed to simulate the transport of electrons through aluminum target. Furthermore, it was also intended to give the complementary investigation of electron backscattering and transmission probabilities, energy and angular dissipations in comparison with the results obtained for positrons.

2. Methods of calculations

The Monte Carlo technique has been applied to the scattering process of keV electrons and positrons in a solid with considerable success. The models adopted in conventional Monte Carlo approaches are based on the simulation of real electron trajectories by the assembly of straight steps of finite length. The simulation repeated a basic series of steps for each of the electron trajectories, which were followed until they either backscattered from the surface or slowed down below 90 eV implanted or transmitted. Incident electrons on the order of 10,000 were used in each simulation run.

In the case of elastic scattering an electron is assumed to move in straight line trajectories at each step with a finite length and constant energy, and then at the end of each step the electron changes the direction of motion according to the Rutherford scattering formula (Seltzer, 1991), which is widely used for describing elastic scattering. For inelastic scattering it is assumed that the electron always loses its kinetic energy at each step

E-mail address: aydina@balikesir.edu.tr

0969-8043/$ - see front matter © 2008 Elsevier Ltd. All rights reserved.
doi:10.1016/j.apradiso.2008.04.022

length by an amount derived from Gryzinski's energy loss equation (Gryzinski, 1965).

The total inelastic scattering cross-section was calculated using both Gryzinskis (1965) and Liljequist's (1983) models, which were successfully applied for positrons in aluminum (Özmutlu and Aydin,1994). In the case of an electron, the upper boundary of integral was taken as $E/2$ instead of E in order to take into account the exchange of final two electrons. Gryzinski's excitation functions were used to describe both core and valance excitations in inelastic processes. The detailed description of the Monte Carlo code and the calculation of cross-sections have been reported elsewhere (Özmutlu and Aydin, 1994; Aydin, 2005).

3. Results and discussion

Fig. 1 shows the variation of total elastic and inelastic cross-sections as a function of incident electron energy calculated by using Gryzinski and Lijequist models in comparison with the results of Penn (1987) for inelastic scattering and Dapor (1996) for elastic scattering. As seen in the figure, the total inelastic cross-section values calculated with Gryzinski and Lijequist models are becoming slightly different at low and high incident electron energies. However, they provide almost the same values at moderate electron energy ranges. For example, while the ratio $\mu_{\text{I Gry}}/\mu_{\text{I Lil}}$ is found to be 1.3379 and 0.9063 for $E = 0.1$ and 30 keV, respectively, it becomes 1.0897 for $E = 1$ keV and 0.9821 for $E = 10$ keV. The total elastic scattering cross-sections

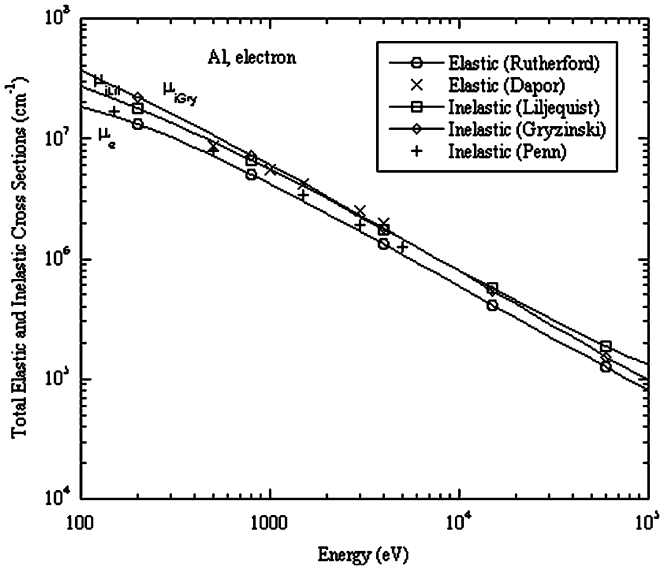

Fig. 1. Variations of elastic and inelastic cross-sections with incident electron energies in comparisons with the theoretical data.

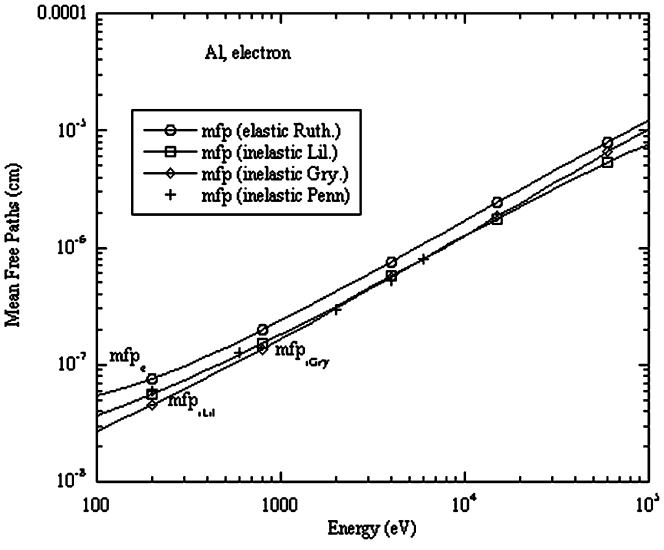

Fig. 2. The mean free paths for elastic and inelastic events in Al.

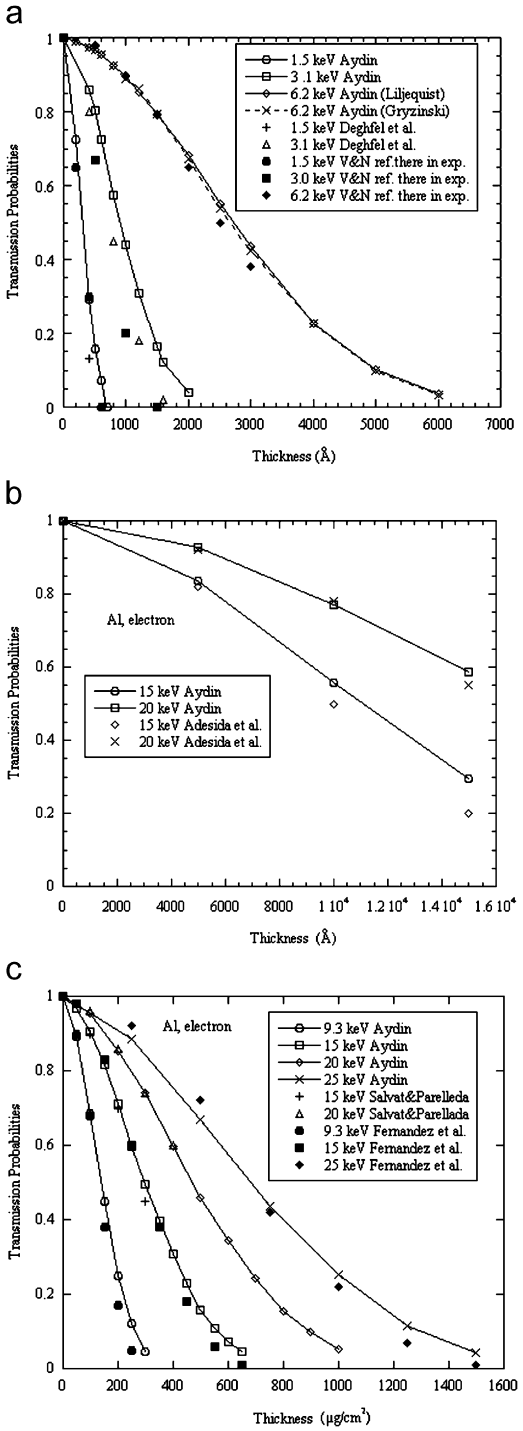

Fig. 3. The transmission probabilities as a function of various energies and thicknesses for Al target in comparison with the theoretical and experimental data.

calculated by the Rutherford scattering model are shown in Fig. 1 along with the results reported by Dapor (1996). It can be seen in Fig. 1 that the values calculated for elastic scattering in the current study are slightly smaller than the results of Dapor (1996) for the whole electron energy ranges investigated in this work. For example, total elastic cross-section of 0.5 keV energetic electrons impinging on aluminum was found to be 7.2118×10^6 cm^{-1}, while the calculation of Dapor was $8.6086 \times 10^6\,cm^{-1}$.

The inelastic electron mean free path plays an important role in surface physics. The inelastic electron mean free path based on the dielectric model as a function of electron energy was studied by Penn (1987) for Cu, Ag, Au and Al. The calculated mean free paths for elastic (mfp_e) and inelastic (mfp_i) events in aluminum are shown in Fig. 2. It is clear that the calculated mean free paths were found to be $mfp_e = 7.5723 \times 10^{-7}$ cm, $mfp_{i\ Lil} = 5.6691 \times 10^{-7}$ cm, $mfp_{i\ Gry} = 5.5619 \times 10^{-7}$ cm, while $mfp_{i\ Penn} = 5.1999 \times 10^{-7}$ cm for 4 keV energy.

In the following section, we present some fundamental results including transmission and backscattering coefficients, the energy and angular distributions of transmitted and backscattered electrons in various thicknesses and semi-infinite aluminum films. The effects of Gryzinski and Liljequist models on the transmission and backscattering probabilities will also be presented for inelastic scattering.

3.1. Slab geometry

The calculated transmission probabilities for various energies and foil thicknesses are shown in Fig. 3, together with the experimental (Valkealahti and Nieminen, 1983 references therein) and other theoretical data (Deghfel et al., 2003; Salvat and Parellada, 1984; Valkealahti and Nieminen, 1983; Adesida et al., 1980). In the inelastic scattering event the effects of Liljequist and Gryzinski models on transmission probabilities are only compared for 6.2 keV energy. The results of Liljequist's and Gryzinski's

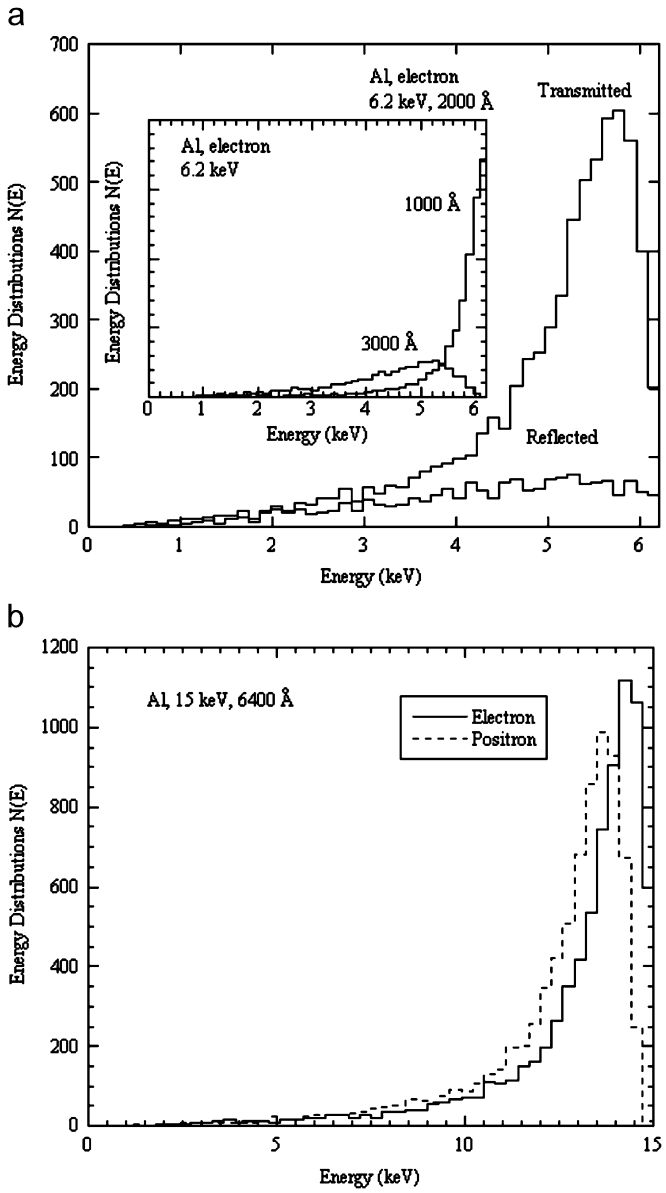

Fig. 4. Theoretical energy distributions of transmitted–reflected electrons and positrons for Al target at various thicknesses.

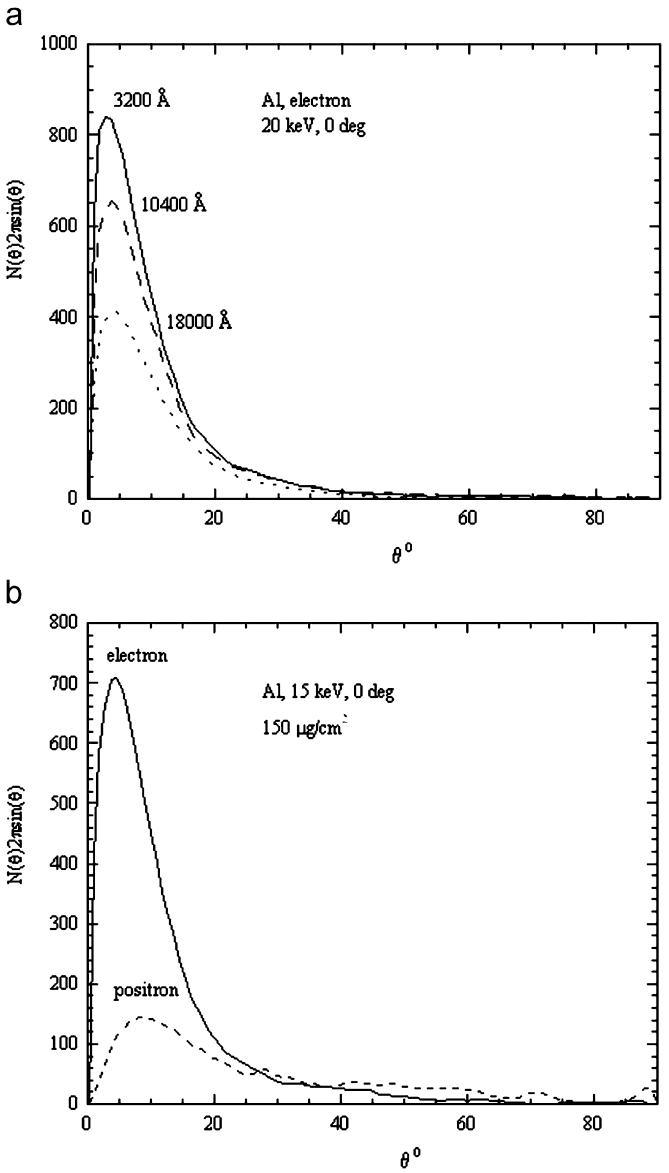

Fig. 5. Theoretical angular distributions of transmitted electrons and positrons in Al target at various thicknesses.

models are consistent with each other and which the experiment in the studied energy range.

Energy distribution of transmitted and reflected electrons for an aluminum target with 2000 Å film thickness at 6.2 keV energy is shown in Fig. 4a. The inset of Fig. 4a shows the dependence of transmitted energy distribution on film thicknesses at 6.2 keV electron energy. The comparison of the energy distributions of transmitted electrons and positrons for aluminum with 6400 Å film thickness at 15 keV energy is shown in Fig. 4b. The angular distributions of transmitted electrons for various target thicknesses at 20 keV are shown in Fig. 5a. Fig. 5b is given to compare the angular distributions of transmitted electrons and positrons for 150 $\mu g/cm^2$ film thickness at 15 keV energy.

3.2. Semi-infinite geometry

The backscattering probabilities of electrons entering into the semi-infinite aluminum target at various incident angles were studied as a function of incident electron energy. Figs. 6a and b show the energy dependence of backscattering probabilities deduced from both using Gryzinski and Liljequist models for electrons entering normally into the semi-infinite aluminum target in comparison with other Monte Carlo results, Deghfel et al. (2003); Liljequist (1998); Dapor (1996); Fernández-Varea et al. (1996); Jensen and Walker (1993); Valkealahti and Nieminen (1984) and available experimental data reported by Massoumi et al. (1993). For 3 keV energy incident on semi-infinite aluminum target at normal angle, the backscattering probabilities were calculated as 0.182 and 0.175 using Liljequist and Gryzinski models for inelastic scattering, respectively. Although these values for 3 keV energy are in high consistency with the calculation of Valkealahti and Nieminen and references therein (1984), they deviate from experimental and other theoretical results above 10 keV due to the total cross-section calculations, which can be adjusted to obtain better agreement.

Fig. 7 shows the calculated backscattering probabilities for electrons entering into the semi-infinite aluminum target at

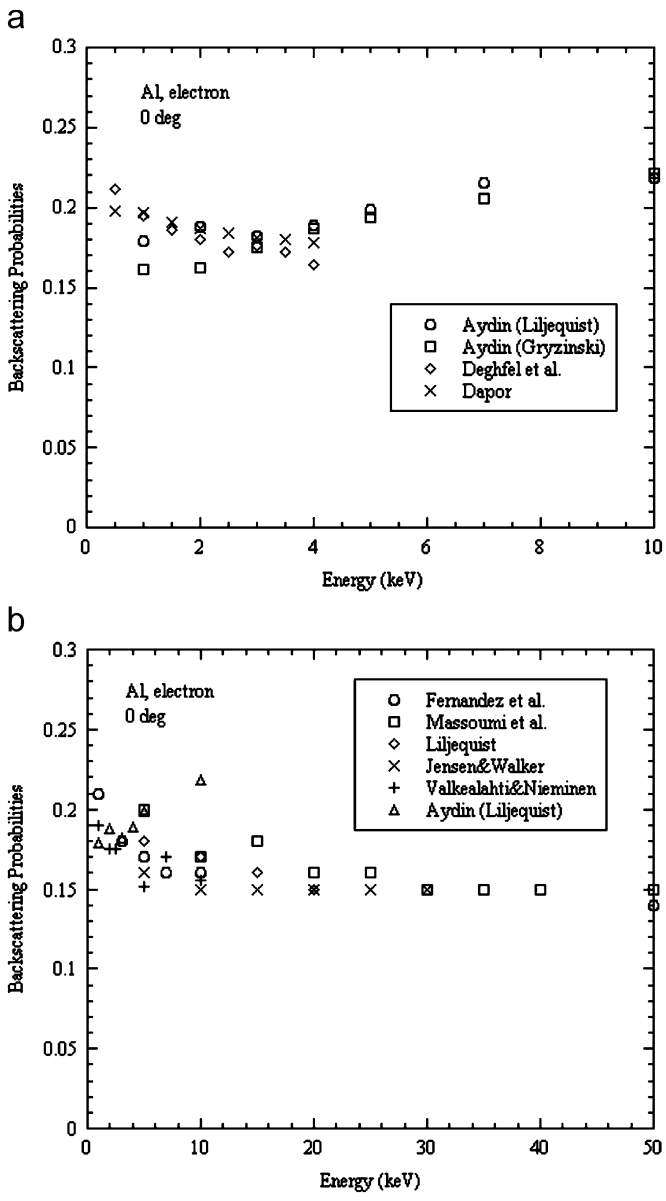

Fig. 6. Comparison of backscattering probabilities for semi-infinite Al.

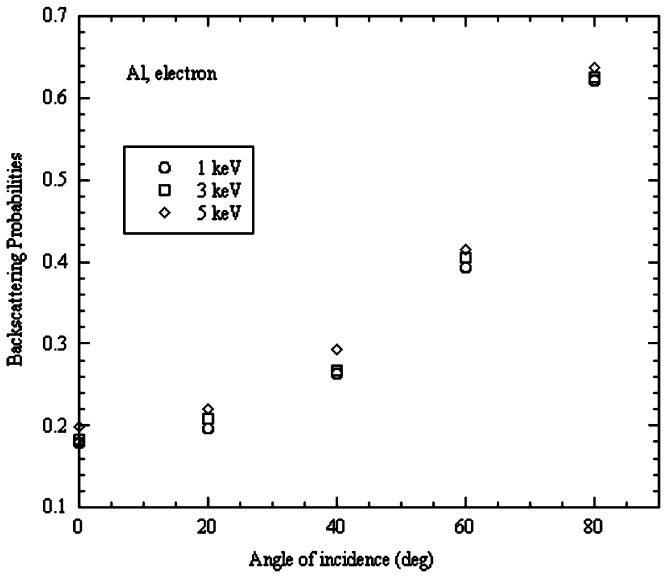

Fig. 7. Backscattering probabilities as a function of electron incoming angles.

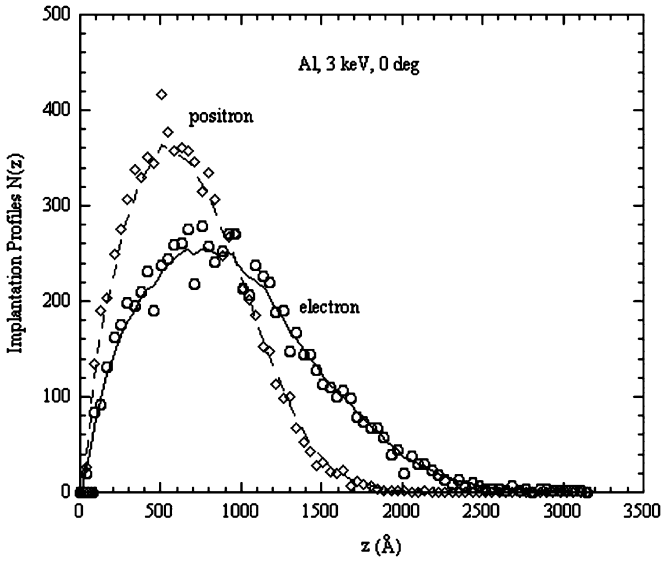

Fig. 8. Typical implantation profiles of electrons and positrons at 3 keV, 0° incident angle in the semi-infinite Al.

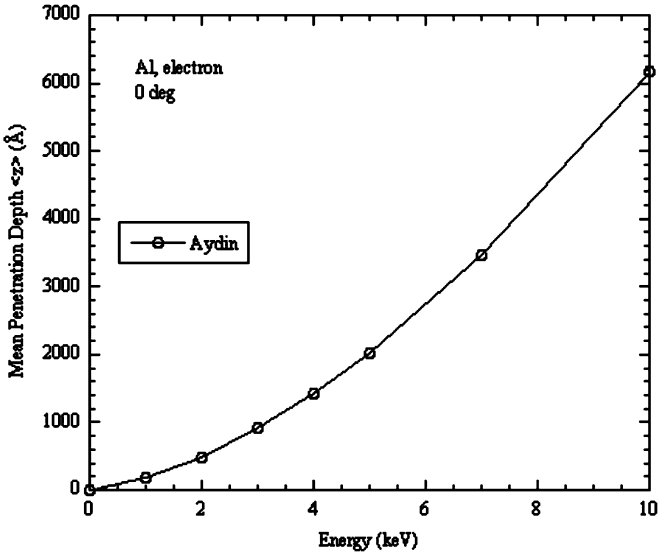

Fig. 9. Mean penetration depths $\langle z \rangle$ as a function of electron energy.

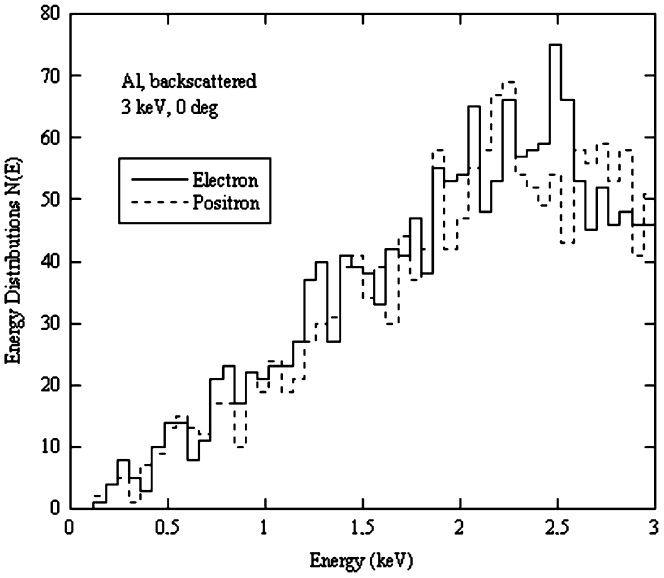

Fig. 10. Theoretical energy distributions of backscattered electrons and positrons from the semi-infinite Al at 3 keV energy and the incident angle of 0°.

various angles in the energy range 1–5 keV. As seen in the figure, the backscattering probabilities strongly depend on the incident angle. It gradually increases as the incident angle increases. It is also seen that the backscattering probabilities increase slightly with the incident electron energy at a fixed incident angle. Fig. 8 shows typical implantation profiles for 3 keV electrons and positrons entering with a 0° angle into the semi-infinite aluminum. The energy and angular distributions of backscattered electrons and mean penetration depths of electrons entering into the semi-infinite aluminum target were also investigated. Fig. 9 shows the calculated mean penetration depth $\langle z \rangle$ of electrons as a function of their energy at normal incident angle. Fig. 10 gives the energy distributions of backscattered electrons and positrons for 3 keV electron energy normally incident onto the semi-infinite aluminum target. The angular distribution of backscattered electrons was also calculated using the current Monte Carlo codes for a semi-infinite aluminum target. Fig. 11 shows angular

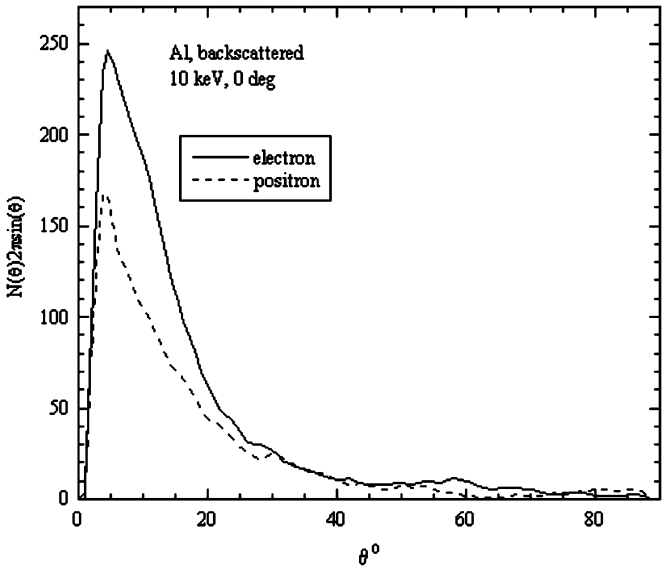

Fig. 11. Theoretical angular distributions of backscattered electrons and positrons from the semi-infinite Al at 10 keV energy and the incident angle of 0°.

distributions of electrons and positrons with 10 keV energy incident onto the target at 0° angle.

4. Conclusions

A Monte Carlo simulation based on screened Rutherford differential scattering cross-section and Gryzinski's approximate energy loss expression was used to calculate the transmission and backscattering probabilities of electrons in the energy range of 25 keV incident upon semi-infinite and finite thickness aluminum targets at various angles. The energy and angular distributions of electrons and the electron implantation profile were investigated and compared with positrons. In general, a good agreement was found between the existing experimental and theoretical data. Although the basic physical mechanisms of interactions of electrons and positrons with solid are reasonably well understood, the intensive research during the last years has been exploited to many exciting developments. In future, we will continue to report new results to seek the improvement in Monte Carlo simulations of transmission and backscattering for keV electrons and positrons incident on different solid targets.

References

Adesida, I., Shimuzu, R., Everhart, T.E., 1980. A study of electron penetration in solids using a direct Monte Carlo approach. J. Appl. Phys. 51, 5962–5969.
Aydın, A., 2005. Monte Carlo calculations of low energy positrons in silicon. Nukleonika 50, 37–42.
Dapor, M., 1996. Elastic scattering calculations for electrons and positrons in solid targets. J. Appl. Phys. 79, 8406–8411.
Deghfel, B., Bentabet, A., Bouarissa, N., 2003. Transmission and backscattering energy distributions of slow electrons from metallic targets. Phys. Stat. Sol. B 1, 136–143.
Fernández-Varea, J.M., Liljequist, D., Csillag, S., Räty, R., Salvat, F., 1996. Monte Carlo simulation of 0.1–100 keV electron and positron transport in solids using optical data and partial wave methods. Nucl Instrum. Methods B 108, 35–50.
Gryzinski, M., 1965. Two-particle collisions I. General relations for collisions in the laboratory system. A305–A321. Two-particle collisions II. Coulomb collisions in the laboratory system of coordinates A322–A335. Classical theory of atomic collisions. I. Theory of inelastic collisions. Phys. Rev. 138, A336–A358.
Jensen, K.O., Walker, A.B., 1993. Monte Carlo simulation of the transport of fast electrons and positrons in solids. Surf. Sci. 292, 83–97.
Liljequist, D., 1983. A simple calculation of inelastic mean free path and stopping power for 50 eV–50 keV electrons in solids. J. Phys. D: Appl. Phys. 16, 1567–1582.

Liljequist, D., 1998. Escape probability of low energy electrons and positrons emitted in random directions beneath a plane solid surface. Nucl. Instrum. Methods B 142, 295–307.
Massoumi, G.R., Lennard, W.N., Schultz, P.J., Walker, A.B., Jensen, K.O., 1993. Electron and positron backscattering in the medium energy range. Phys. Rev. B 47, 11007–11018.
Özmutlu, E.N., Aydin, A., 1994. Monte-Carlo calculations of 50 eV–I MeV positrons in aluminum. Appl. Radiat. Isot. 45 (9), 963–971.
Penn, D.R., 1987. Electron mean free path calculations using a model dielectric function. Phys. Rev. B 35, 482–486.
Salvat, F., Parellada, J., 1984. A simple Monte Carlo calculation of kilovolt electron transport. J. Phys.D: Appl. Phys. 17, 185–201.
Seltzer, S.M., 1991. Electron-photon Monte-Carlo calculations: the ETRAN code. Appl. Radiat. Isot. 42 (10), 917–941.
Valkealahtij, S., Nieminenj, R.M., 1983. Monte Carlo calculations of keV electron and positron slowing down in solids. Appl. Phys. A 32, 95–106.
Valkealahti, S., Nieminen, R.M., 1984. Monte Carlo calculations of keV electron and positron slowing down in solids II. Appl. Phys. A 35, 51–59.